Asian Journal of Nanoscience and Materials 4 (2021) 290-308

SPC

Asian Journal of Nanoscience and Materials

Journal homepage: www.ajnanomat.com

Original Research Article

The ability of Tragopogon graminivorous DC *edible* medicinal plant for optimum synthesis of zinc oxide green nanoparticles and evaluation of antibacterial properties of its extract and nanoparticles

Marzieh Naderi, Ghazaleh Kouchakzadeh*

Department of chemistry, Khorramabad Branch, Islamic Azad University, Khorramabad, Iran

ARTICLE INFORMATION

Received: 6 July 2021
Received in revised: 9 August 2021
Accepted: 16 August 2021
Available online: 26 September 2021

DOI: 10.26655/AJNANOMAT.2021.4.5

KEYWORDS

Tragopogon graminifolius DC
Edible-medicinal plant
Zinc oxide nanoparticles
Antibacterial properties
Optimal conditions

ABSTRACT

In recent years, the green synthesis of nanoparticles has become an environment-friendly method developed significantly. In this method, plant extract as a reductive and stabilizing agent plays a key role in the synthesis of nanoparticles. In this study, the optimum conditions for the green synthesis of ZnO nanoparticles are investigated using the extract of Tragopogon graminivorous DC edible-medicinal plants. Also, the antioxidant effect of the plant extract and antibacterial properties of nanoparticles and extract are evaluated. After preparation of the aqueous extract, its antioxidant properties were evaluated by the DPPH method. Then, parameters such as pH, zinc acetate dihydrate concentration, the volume of plant extract, temperature, and time were optimized. The green nanoparticles were characterized by UV-Vis, FT-IR, X-ray diffraction, and scanning electron microscope techniques. Finally, antibacterial properties of extract and biosynthesized ZnO nanoparticles were investigated. The results of the DPPH method showed that plant extract can be used as a reductive agent. Overall, it can be said that the presence of various chemical compounds that have caused the antioxidant properties of plant extract demonstrate the ability of the extract as a source of natural antioxidants. Also, plant extract and nanoparticles can be regarded as antibacterial agents.

Corresponding author, email: ghkouchakzadeh@khoiau.ac.ir (G. Kouchakzadeh).
Tel.: +98-66-33120399.

Graphical Abstract

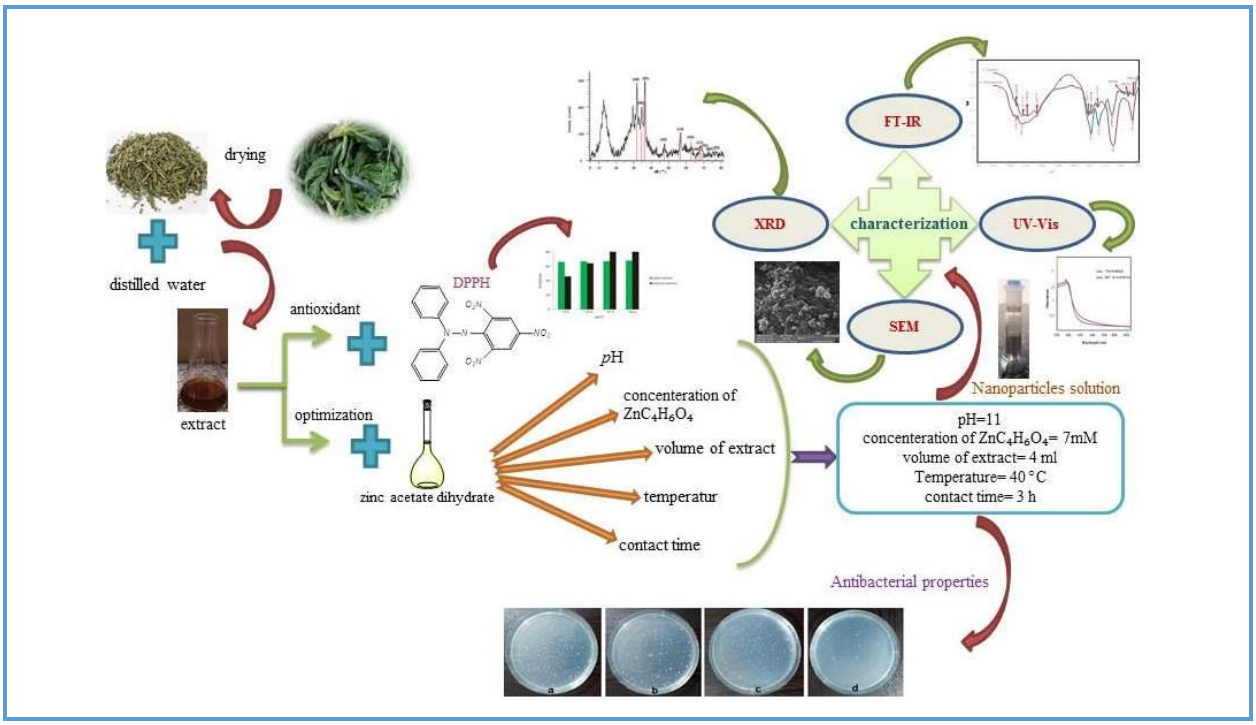

Introduction

In recent years, green synthesis has played a significant role in nanotechnology and green synthesis of metal and metal oxide nanoparticles [1]. Nanotechnology is the science of production and application of materials on a very small (nanometric) scale. The importance and attractiveness of the nanoscale are attributed to the different properties of materials in this scale compared to other scales, even micro. Nanoparticles have various chemical and physical properties due to their very small size and very high surface-to-volume ratio. Traces of this emerging science can be seen in various fields including, food, medicine, health-cosmetics, agriculture, and electronic devices [2]. Synthesis of nanoparticles by physical and chemical methods and using hazardous and toxic chemicals cause pollution and environmental damage. According to previous studies, nanoparticles, due to their very small size, may enter the body and digestive system of humans and other animals through the nose and mouth, which might result in damaging the tissues [3]. Some researchers have shown that high concentrations of ZnO nanoparticles can damage kidney tissue [4]. Toxic doses of ZnO nanoparticles can increase the production of reactive oxygen species and inhibit the antioxidant activity, thereby causing inflammation and damage to liver tissue [5]. Given the concerns regarding the harm to human and animal health caused by producing nanoparticles through chemical methods and environmental damage, the method of green synthesis of nanoparticles has received much attention. In this method, plants and microorganisms are used to prepare metal and metal oxide nanoparticles as alternatives to chemical methods [6–7]. This method, which is used to produce safe and eco-friendly nanoparticles, has been the subject of intense

research in the field of nanotechnology. In green synthesis, plants and microorganisms are used as reducing agents for the production of nanoparticles. This reducing agent has a significant effect on the morphology of particles such as size, physicochemical properties, and shape. Another noteworthy point in this regard is that morphology affects the properties of nanoparticles [8, 9].

Carboxylic acid groups, amines, proteins, carbohydrates, phenols, terpenes, and vitamins found in the extract of plants play an influent role in biosorption and bioreduction processes involved in the synthesis of nanoparticles [10]. Accordingly, evaluation of antioxidant properties of plants may indicate the presence of phenolic compounds in them. These compounds demonstrate the plant's ability to bioreduction and produce nanoparticles. Phenolic compounds have numerous biological effects such as antioxidant, antiviral, antibacterial, anti-inflammatory, and anti-allergic properties and suppress the growth of cancer cells [11]. Different parts of plants and various microorganisms are used as reducing agents in the green synthesis of ZnO nanoparticles [12, 13]. Zinc oxide is used as an additive in various materials and products such as plastics, ceramics, glass, cement, ointments, adhesives, paints, catalysts and foods [14]. In this research, the ZnO nanoparticles were synthesized in the presence of an aqueous extract of the medicinal plant Tragopogon graminifolius DC. Water solvent has an advantage over organic solvents due to their availability, low price, and non-toxicity. Tragopogon graminifolius DC is a biennial herb of 30-125 cm height and is from the family Asteraceae [15]. This plant, which grows in the West of Iran, is known as "Sheng". Tragopogon is made of two Greek words: tragos (i.e., goat) and pogon (i.e., beard) [16]. In traditional medicine, this plant is used to treat rheumatism, poisoning, wound healing, skin diseases, gastric ulcers, and healed severed nerve [17, 18]. The effects of this plant have been also confirmed by several studies [18–22]. Tragopogon graminifolius DC extract can have hepatoprotective effects [23]. So far, several studies have been conducted on the properties of different species the genus Tragopogon [24, 25]. According to these studies, these species contain flavonoids such as luteolin, isovitexin, vitexin, and vicenin [26, 27], as well as phenolic compounds such as p-coumaric acid, catechin, gallic acid, ferulic acid, and caffeic acid [28]. These acids have antioxidant activity and thus fight free radicals that cause cancer. In this research, the green synthesis of ZnO nanoparticles was performed using the aqueous extract of Tragopogon graminifolius DC, which is less reported in another study. To this end, first, the antioxidant properties of the aqueous extract of the plant were evaluated to confirm the presence of a reducing agent. Then, the factors affecting the synthesis of zinc oxide nanoparticles such as pH, zinc acetate concentration, extract concentration, temperature and time, as well as antimicrobial properties of the extract and nanoparticles were investigated.

Experimental

Materials and methods

Zinc acetate dihydrate, sodium hydroxide, phosphoric acid, acetic acid, boric acid, and other chemical materials used in the study were purchased from Merck Company. Acids and sodium hydroxide were used to prepare Britton - Robinson buffer [29] and control pH. The other devices and their manufacturers used in this study are as follows: XRD (D8ADVANCE, Bruker, Germany); FT-IR (Spectrum RXI, Perkin Elmer, Germany); V-Visible (Lambda 25, Perkin Elmer, Germany); SEM (MIRA3 FESEM,

TESCAN, Czech republic); Heater-Stirrer (ARE, VELP, Italy); Centrifuge (ALC 4232, Italy); Oven (Binder, Germany). Fresh leaves of Tragopogon graminifolius DC were collected from some plains in the south of Khorramabad, Iran.

Preparation of plant leaf aqueous extract

The leaves of Tragopogon graminifolius DC were washed twice with distilled water and air-dried at room temperature. Then, the dried leaves were crushed into small pieces. About 5 g of the dried plant was mixed with 100 mL of distilled water. The solution was then stirred for 40 min in a batch of water at 40 °C. After cooling extract, it was filtered through Whatman filter paper. To separate the plant residues, the solution was centrifuged at 5000 rpm for 10 min. Finally, the sample was stored in the refrigerator for later use.

Evaluation of the antioxidant activity of Tragopogon graminifolius DC extract

The antioxidant activity of Tragopogon graminifolius DC extract was measured by the DPPH method to evaluate its scavenging ability of free radicals. This experiment was performed following the method proposed by Brand-Williams [30]. The 2, 2-diphenyl- 1-picrylhydrazyl Hydrate (DPPH) is a stable free radical that has the lone pair electron on one of its nitrogen bridge atoms. To evaluate the amount of free radical trapping, 0.0634 mM DPPH solution in 95% methanol was prepared. First, the absorption of DPPH radical, known as the control solution, was measured by UV-Vis spectroscopy alone at a wavelength of 517 nm. All measurements were performed at room temperature. About 3.9 mL of the main solution of DPPH was added to different concentrations of plant extract (12.5, 25, 37.5, and 50 µg/mL) and ascorbic acid as a standard sample. The solutions were kept in a dark place. For all samples, the decrease in the absorption peak at 517 nm was determined for 30 min and the antioxidant activity percentage was evaluated using the Equation 1.

$$\%\ inhibition\ = \frac{(A_c - A_s)}{A_c} \times 100 \qquad (1)$$

where A_c and A_s are the absorbances of a solution of DPPH at t=0 min and the absorbance of the sample after 30 min, respectively [31–33].

Synthesis of ZnO nanoparticles by plant extract

Synthesis of ZnO nanoparticles from Tragopogon graminifolius DC extraction was carried out under different conditions. The effects of pH, the concentration of zinc acetate dihydrate solution, the volume of plant extract, temperature, and contact time of zinc acetate dehydrate solution with plant extract were evaluated and optimal values were obtained.

The effect of pH on green synthesis of ZnO nanoparticles

First, 5 mL of 1 mM zinc acetate dihydrate aqueous solution at different pH levels (2, 5, 7, 9, and 11) were added to 2 mL of plant extract. Then, the mixture was kept in dark at room temperature for 3 h. The pH control was performed using Britton-Robinson buffer. After 3 h, the solutions were centrifuged at 5,000 rpm for 10 min to separate the precipitate. In the next step, UV-Vis spectrophotometry was used in the range of 350-700 nm. The maximum value of the absorption was observed in pH=11 and it was reported as the optimum pH.

The effect of concentration of zinc acetate dihydrate on green synthesis of ZnO nanoparticles

Different concentrations of zinc acetate dihydrate aqueous solution (1, 3, 5, 7, and 8

mM) were prepared considering the optimal pH. About 5 mL of zinc acetate dihydrate aqueous solution with different concentrations at pH=11 were added to 2 mL of plant extract and the mixture was kept in dark at room temperature for 3 h. Then, the solutions were centrifuged at 5,000 rpm for 10 min to separate the precipitate. Finally, UV-Vis spectrophotometry was performed in the range of 350-700 nm, which revealed the maximum absorption. The results of UV-Vis spectrophotometry showed that optimal the concentration of salt is 7 mM.

The effect of the plant extract's volumes on the green synthesis of ZnO nanoparticles

To evaluate the effect of different volumes of Tragopogon graminifolius DC extract (1, 2, 3, 4, 5 mL) on green synthesis of ZnO nanoparticles with previous optimal conditions, 5 mL of 7 mM zinc acetate dihydrate aqueous solution at pH=11 were added to different volumes of the plant extract. The mixture was kept in dark at room temperature for 3 h. After centrifuging at 5,000 rpm for 10 min, UV-Vis spectrophotometry was used in the range of 350-700 nm. The maximum absorption was observed in the volume of 5 mL.

The effect of temperature on green synthesis ZnO nanoparticles

About 5 mL of 7 mM zinc acetate dihydrate aqueous solution were added to 4 mL of plant extract. They were kept in dark at different temperatures (4, 20, 30, 50, and 60 °C) for 3 h. After centrifuging, UV-Vis spectrophotometry was used in the range of 350-700 nm, at which the maximum absorption was obtained. The optimal temperature was observed at 40 °C.

The effect of time on green synthesis of ZnO nanoparticles

To study the effect contact time of zinc acetate dihydrate solution with plant extract on green synthesis of ZnO nanoparticles with previous optimal conditions, 5 mL of 7-mM zinc acetate dihydrate aqueous solution was added to 5 mL of plant extract. They were kept in dark at different lengths of time (30-240 min). Then, the solutions were centrifuged at 5,000 rpm for 10 min and UV-Vis spectrophotometry was used in the range of 350-700 nm. The optimal time was found to be 180 min.

The optimal green synthesis of ZnO nanoparticles

After obtaining the optimal conditions in the experiments, ZnO nanoparticles were synthesized by Tragopogon graminifolius DC edible-medicinal plant accordingly. The synthesized ZnO nanoparticles were characterized by UV-Vis, FTIR, XRD, and SEM techniques. Optimal conditions of biosynthesis ZnO nanoparticles included pH=11, $AgNO_3$ concentration = 7 mM, extract volume = 5 mL, temperature = 40 °C, and time = 180 min.

The study of antibacterial properties of the extract and nanoparticles

In this step, the antibacterial potential of the nanoparticles and extract against Staphylococcus Aureus (ATCC) and Escherichia coli (ATCC) was examined. For this purpose, first, Luria-Bertani (LB) medium was synthesized and sterilized. Then, different weights of samples (0.001, 0.01, 0.05, 0.10, and 0.15 g) were added to 10 mL of LB medium and suspension solutions were prepared with different concentrations of nanoparticles (0.01, 0.1, 0.5, 1, and 1.5%). These media were sterilized in an automatic autoclave at 121 °C and a pressure of 15 lb for 15 min and then were refrigerated. About 34 g of Mueller-Hinton agar culture medium in 1 liter of distilled water was used to prepare fresh culture of Staphylococcus

aureus (S. aureus) and Escherichia coli (E. coli) bacteria. To prepare the suspension, one loop of each microbial strain was incubated in 20 mL of culture medium in a sterilized flask, and bacteria were cultivated until the concentration reached 105 cells/mL. Next, 2 mL of diluted bacteria was added to the culture medium, nanoparticles, and plant extract. The same steps were used to provide positive control but no nanoparticles were added. Also, a culture medium without bacterial was considered as negative control [34]. All samples were grown for 24 h in an incubator at 37 °C under continuous shaking at 250 rpm. After this time, the concentrations of samples that contained bacterial cells mixed with nanoparticles and bacterial cells mixed with plant extract were measured by OD_{600} [35, 36].

Result and Discussion

The synthesis of nanoparticles is a very interesting field of research regarding their unusual chemical and electrical properties. Metal nanoparticles such as zinc oxide have attracted the attention of researchers because of their antibacterial properties, chemical stability, and high catalytic activity, as well as their ability to absorb and reflect ultraviolet rays. These nanoparticles were used in the cosmetics and ceramics industries and in producing wound adhesives. Physical methods of synthesis of nanoparticles are expensive and chemical techniques usually performed using toxic reagents. In comparison, the green synthesis of nanoparticles is very low cost and can be used as a replacement for physical and chemical methods [33, 37–39].

Evaluation of antioxidant properties

Different parts of most plants are rich in phenolic compounds, which are widely used by the plant itself and in industrial products [11, 40, 41]. Usually, plant extracts that contain phenolic compounds have good antioxidant properties. Plants are natural antioxidants that play an effective role in human health. When an imbalance occurs between the generation and diminution of reactive oxygen species, these species cannot be eliminated by the antioxidants [42], thereby antioxidants are effective in preventing diseases [24]. Because living organisms have different defense mechanisms against free radicals, cancer, heart attack, and nerve damage can occur if antioxidant defenses are inadequate. In this research, DPPH free radicals were used to evaluate the antioxidant properties of plant extract. According to Figure 1, the maximum DPPH free radical scavenging for aqueous extract of Tragopogon graminifolius DC is 25 µg/mL.

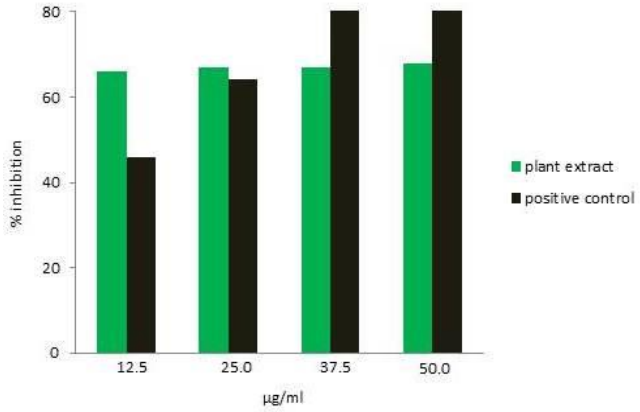

Figure 1. Demonstration of DPPH free radical scavenging activity by Tragopogon graminifolius DC extract compared to a positive control (ascorbic acid)

The percentage of DPPH free radical scavenging at high concentrations declines relative to ascorbic acid. The aqueous extract of Tragopogon graminifolius DC that has antioxidant properties is a donor molecule. Also, the plant extract denotes a hydrogen atom to DPPH free radical, and the color of the

mixture DPPH free radical and extracts change from purple to yellow. In this respect, the wavelength of the mixture decreases and it is radically reduced to DPPH-H molecule [43, 44]. Figure 2 presents the conversion of DPPH free radical to a DPPH-H. Therefore, it can be said Tragopogon graminifolius DC aqueous extract at medium concentration can be a good reducing agent.

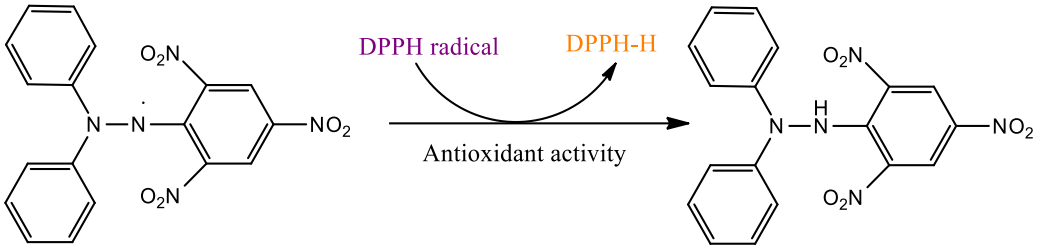

Figure 2. Schematic representation of DPPH free radical scavenging and its conversion to DPPH-H

The structure of flavonoids in genus Tragopogon has been predicted in previous studies [26, 27]. The flavonoids in Tragopogon graminifolius DC extract play a role of capping agent. The synthesis mechanism of ZnO nanoparticles using flavonoids has been proposed in Figure 3. The results of previous studies have been considered in proposed mechanism [45–47]. Figure 3 shows zinc ions are capped by secondary metabolites of Tragopogon graminifolius DC extract. Then they were hydrolyzed to remove flavonoids. In this mechanism, ZnO nanoparticles were produced by heating of $Zn(OH)_2$ intermediates [48].

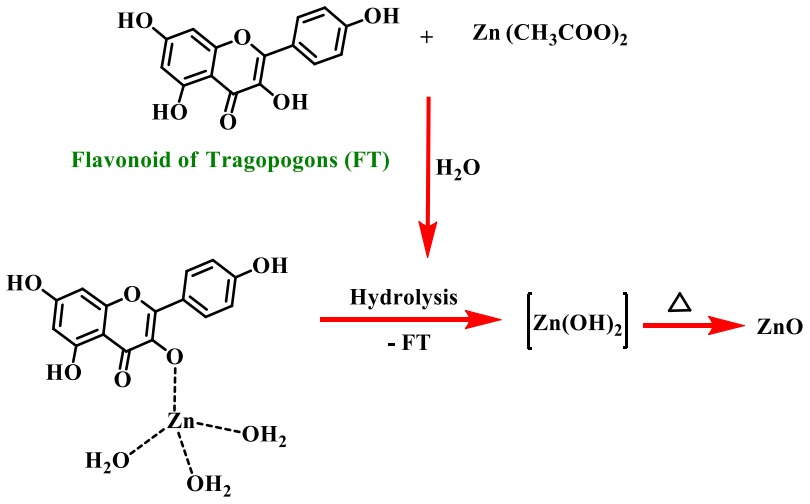

Figure 3. Proposed mechanism of synthesized ZnO nanoparticles by Tragopogon graminifolius DC extract

Optimization of ZnO bionanoparticles

Optimization of nanoparticles influences their properties and morphology. Therefore, in this research, optimization of different parameters of green synthesis of ZnO nanoparticles was evaluated. In the green synthesis of ZnO nanoparticles, pH can influence the formation of nanoparticles. In [49], it was reported that ZnO nanoparticles are

usually soluble well in low pH ranges while they segregate partially in high pH levels. Because pH can affect the electrical charge of biomolecules, it may change the reduction ability of these molecules and the growth of nanoparticles [50]. The UV-Vis spectrum in Figure 4 shows a strong bandwidth in the range of 330-450 nm. According to Figure 4, pH can affect the size of ZnO nanoparticles, leading to the shift of the main peak [51]. According to the mentioned points, in low pH ranges such as 2 and 5, the main peak was not observed in the range of 330-450 nm. The main bandwidth peak appeared at pH=7-11, but its location is shifted with chanting the pH.

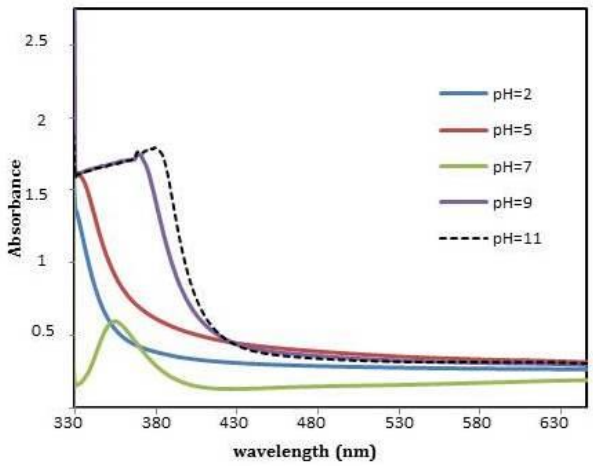

Figure 4. The effect of different pHs on the synthesis of ZnO nanoparticles by Tragopogon graminifolius DC extract

When pH increases from 5 to 11, the main peak shifts to a larger wavelength, and the formation rate of nanoparticles can increase. As a result, coarser nanoparticles can form [49]. According to other studies [52, 53], in a neutral and alkaline environment, hydroxyl groups may present on the sample surface and intermediate molecule $Zn(OH)_2$ may form. The optimal pH depends on the stabilizing agent. Spectroscopic observations show the optimal pH for the biosynthesis of ZnO nanoparticles by Tragopogon graminifolius DC edible-medicinal plant is pH=11.

Another factor influencing the biosynthesis of ZnO nanoparticles is the concentration of zinc acetate dihydrate. The concentration of salt can control the rate of nucleation. The UV-Vis spectrum in Figure 5 shows the variations of absorbance versus concentration of the zinc acetate dihydrate. According to this figure, it can be claimed that at high salt concentration, the formation of ZnO nanoparticles is reduced. At high zinc acetate concentrations, due to a large amount of Zn^{2+} ions, the zinc complexes such as $Zn_2(OH)^{3+}$ and $Zn_2(OH)_6^{2-}$ may form [54]. Also, despite a large number of acetate ions, zinc ions may be extremely attracted by these anions, leading to the formation of zinc alkoxide [55]. According to Figure 5, different concentrations of zinc acetate dihydrate (1, 3, 5, 7, and 8 mM) can change the main peak condition. When the salt concentration increased from 1 mM to 7 mM, the rate of reduction increased, as well. But for 8 mM zinc acetate, the main peak decreases strongly. As mentioned earlier, the presence of other species in solution can affect the peak intensity of ZnO nanoparticles. Therefore, the optimal concentration of zinc acetate dihydrate in biosynthesis ZnO nanoparticles was 7 mM.

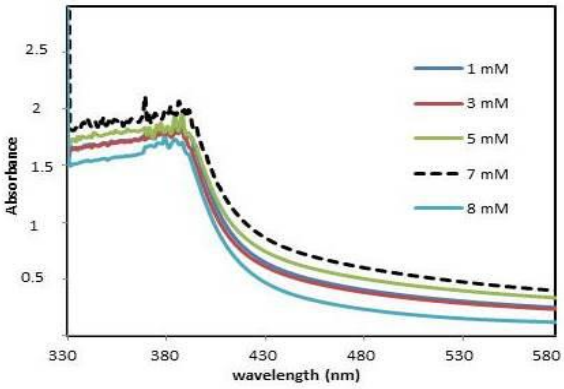

Figure 5. The effect of different concentrations of zinc acetate dihydrate on the synthesis of ZnO nanoparticles by Tragopogon graminifolius DC extract

In this study, the effect of different volumes of Tragopogon graminifolius DC extract (1, 2, 3, 4, and 5 mL) was evaluated. As seen in Figure 6, by increasing the volume of plant extract, the rate of reduction was increased. Certainly, with increasing the volume of plant extract, the main peak slowly shifted to a larger wavelength. Due to the concentration effect of plant extract on optical transmittances, the color of solutions becomes darker [56]. According to another study [56], at the high concentrations of plant extract, there is an agglomeration possibility of nanoparticles; therefore, high concentrations of the extract were not used. Moreover, studying the antioxidant properties of Tragopogon graminifolius DC extract indicated that at a medium concentration of extract, the amount of antioxidant properties is higher than ascorbic acid (Figure 6). Tragopogon graminifolius DC extract is a good reducing agent at medium concentrations. The optimal volume of plant extract in biosynthesis ZnO nanoparticles was 5 mL.

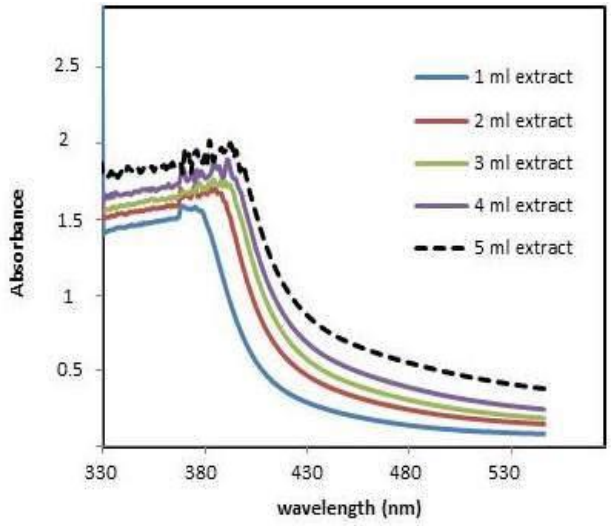

Figure 6. The effect of different volumes of the plant extract on the biosynthesis of ZnO nanoparticles

Temperature is another important factor with an effective role in the biosynthesis of ZnO nanoparticles. In this research, by increasing temperature from 4 to 40 °C, the reduction rate of metal ions increased, as well (Figure 7). At higher temperatures, $Zn(OH)_2$ can be easily converted to ZnO [54]. It is of note that the reaction rate depends on the temperature. Here, the reaction rate has reduced at 50 and 60 °C, suggesting that plant extract as a reducing agent may become unstable at high temperatures [49].

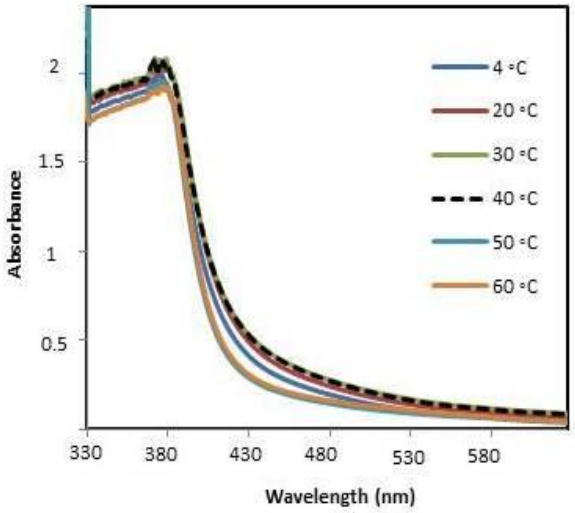

Figure 7. The effect of different temperatures on the synthesis of ZnO nanoparticles by Tragopogon graminifolius DC extract

The contact time of plant extract as reducing agent and zinc acetate dihydrate aqueous solution is another influencing factor. When plant extract was added to 7 mM zinc acetate dihydrate aqueous solution, the color of the solution containing nanoparticles changed. The change in the color was from light brown to dark brown. When the color of solutions containing nanoparticles remains unchanged for a long time, it suggests the dispersion of ZnO nanoparticles without agglomeration [25]. According to Figure 7, absorption intensity increases as temperature rises. The high absorption intensity expresses that nanoparticle formation improves with increasing the synthesis time from 30 min to 90

min. The absorption intensity is the same in 90 min and 120 min and for 180 min and 240 min. The optimal time for the biosynthesis of ZnO nanoparticles was 180 min (Figure 8).

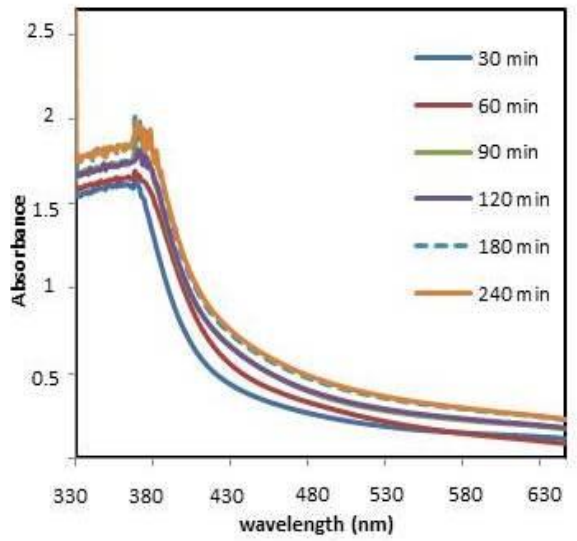

Figure 8. The effect of different times on synthesis of ZnO nanoparticles by Tragopogon graminifolius DC extract

Characterization of ZnO green nanoparticles

After optimizing the parameters, ZnO nanoparticles were synthesized in optimal conditions by Tragopogon graminifolius DC extract. Figure 9 shows UV-Vis spectra of these nanoparticles and aqueous extract. The maximum absorbance for synthesized nanoparticles was observed at 380 nm. The color change of the solution indicates the formation of nanoparticles. This color change was due to the surface plasmon resonance of ZnO nanoparticles, which is one of the distinguishing properties of nanoparticles from large-scale materials. The surface plasmon resonance occurs when light entering a nanoparticle with a specific frequency equals the surface plasmon frequency [25].

XRD spectrum of ZnO nanoparticles is presented in Figure 10. The XRD pattern of synthesis of ZnO nanoparticles indicates a hexagonal structure in agreement with the Joint Committee on Powder Diffraction Standards (JCDS) database (card No. 36-1451) [57-58]. The sharp and intense peaks of this XRD pattern demonstrate that the ZnO nanoparticles were synthesized by plant extract and almost have spherical shapes.

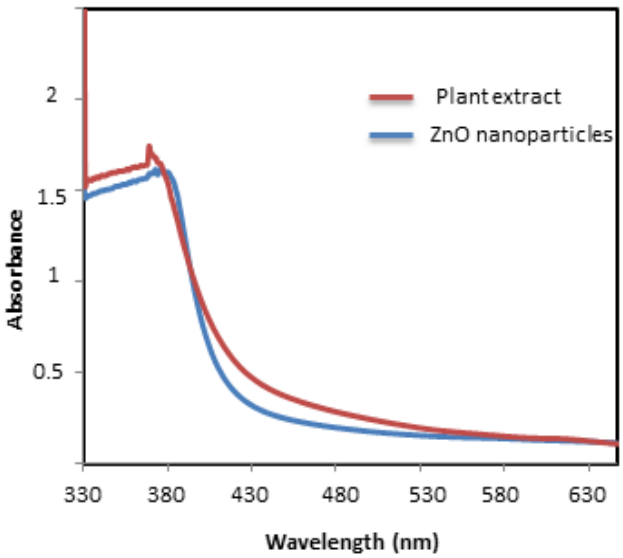

Figure 9. The UV-Vis spectrum of ZnO nanoparticles synthesized from Tragopogon graminifolius DC extract

The peaks of synthesized green nanoparticles appeared at 2θ angles of 31.7°, 34.6°, 36.4°, 47.75°, 57.7°, 63.9°, 66.9°, 67.1°, 68.1° , 72.55°, and 76.85°, which correspond to (100), (002), (101), (102), (110), (103), (200), (112), (201), (004), and (202) planes, respectively. The average crystallite size was estimated using the Debye-Scherrer formula, as follows:

$$D = \frac{0.9\,\lambda}{\beta\,cos\theta} \qquad (2)$$

Where D is the average crystallite size, λ, β, and θ is the wavelength of X-ray used (1.540598Å), the angular peak width at half

maximum, and Bragg's diffraction angle, respectively.

ZnO nanoparticles are important materials because of their optical and electrical properties. These nanoparticles are semiconductor crystals that have a wide bandgap and large excitation energy. Therefore, ZnO nanoparticles are used in UV absorption, UV light emitters, and as photocatalyst [57, 58]. The average size of ZnO nanoparticles was 11.15 nm, which was calculated from the width of peak (101) reflection. At low angles, a wide peak appeared which can be related to the phase of plant extract.

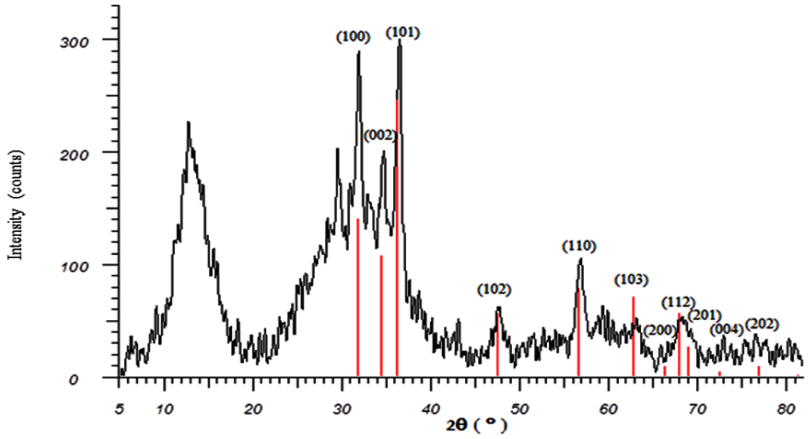

Figure 10. The XRD pattern of ZnO nanoparticles synthesized from Tragopogon graminifolius DC extract

SEM is applied to examine the surface morphology and estimates the shapes of nanoparticles [59]. The SEM images of synthesized ZnO nanoparticles are presented in Figure 11. Using Tragopogon graminifolius DC extract as a reducing agent, we obtained a heterogeneous powder with an average size of 3.2-23.2 nm, suggesting that the morphology of ZnO nanoparticles changes from spherical particles to big polyhedral particles [59].

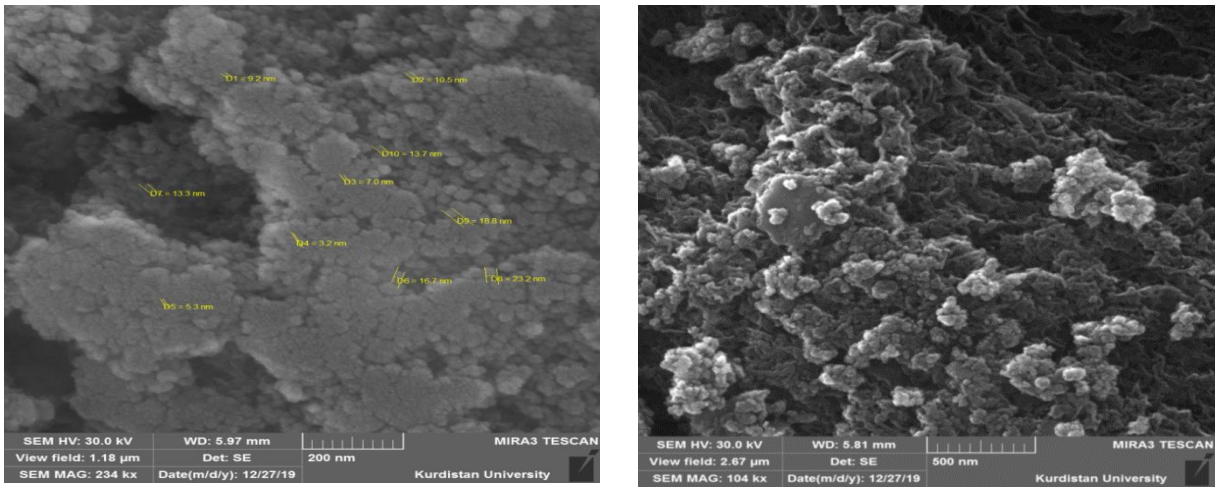

Figure 11. The SEM images of ZnO nanoparticles synthesized by Tragopogon graminifolius DC extract

FT-IR spectrum is used to identify effective bonds and biomolecules that may be able to produce ZnO nanoparticles by Tragopogon graminifolius DC extract. Figure 12 depicts the FT-IR spectrum of biosynthesized ZnO nanoparticles and Tragopogon graminifolius DC extract. This spectrum was obtained in the range of 4000 to 400 cm^{-1}. The peak in the range of 561 cm^{-1} is due to ZnO nanoparticles [59–61]. The other peaks at 3438, 3290, 3185, 2930, 1595, 1419, and 1044 cm^{-1} correspond to the FT-IR of Tragopogon graminifolius DC extract. In the FT-IR of Tragopogon graminifolius DC extract, the absorption band in the range of 3436-3273 cm^{-1} is due to the O-H stretching vibration. The peak in the range 3185 cm^{-1} probably corresponds to the C-H stretching vibration or C = C band, which is related to the presence of flavonoids. The peaks obtained at -1592 cm^{-1} can belong to the C = O band. The absorption band between 1600-1405 cm^{-1} may be indexed to the C = C bending vibration, which can be due to the presence of terpènes. The peaks around 767-669 cm^{-1} can correspond to aromatics rings [60, 61]. FT-IR analysis indicated that ZnO nanoparticles could be surrounded by biomolecules. Comparing two spectra in Figure 11 indicates that plant extract plays a role in reducing agents for synthesizing nanoparticles [49].

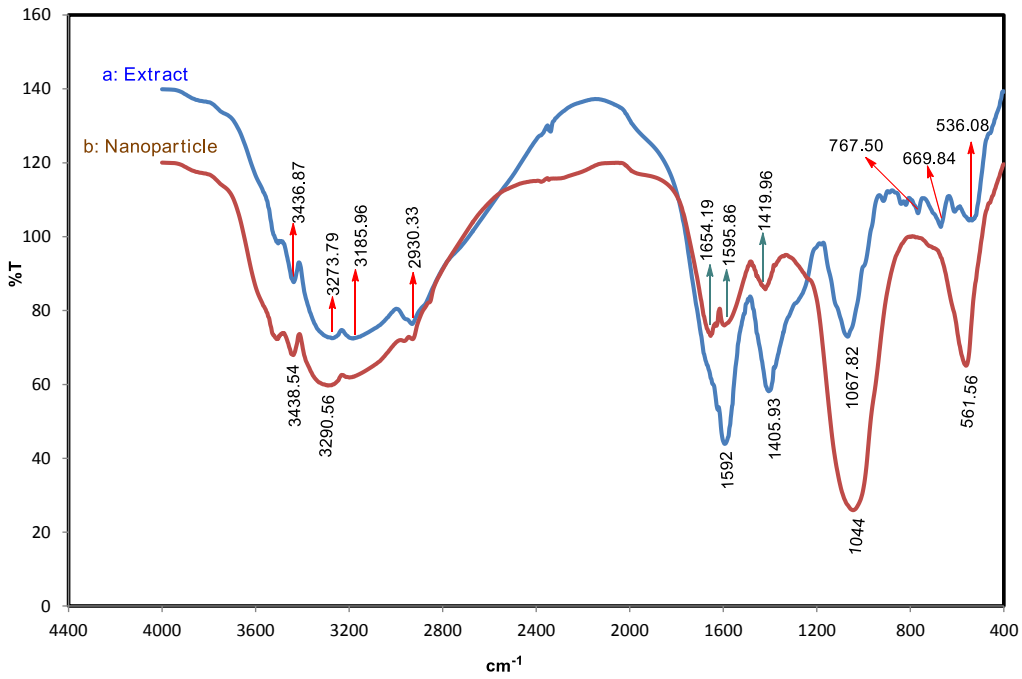

Figure 12. The FT-IR spectrum of ZnO nanoparticles synthesized by Tragopogon graminifolius DC extract

Optical properties of ZnO nanoparticles

Semiconductors have a forbidden band, although with low energy. Therefore, thermal energy, even at room temperature, can transfer some of the electrons and create a limited amount of electrical conductivity [62].

The optical bandgap of synthesized ZnO nanoparticles at different times and temperatures can be determined using Figures 7 and 8. This bandgap can be compared with the direct bandgap of ZnO (λ≈376 nm; 3.3 eV) [61–64]. Figure 13 shows the absorption edge wavelengths at different times and

temperatures. The optical band gap (E_g) was calculated as:

$$E_g\ (eV) = \frac{h.c}{\lambda_{absorption}} \approx \frac{1241}{\lambda_{absorption}} \qquad (3)$$

Where E_g is expressed in eV, $\lambda_{absorption}$ is the absorption wavelength of synthesized ZnO nanoparticles that shows the absorption edge wavelength in nm, and h and c are Planck's constant and the velocity of light, respectively [64–67].

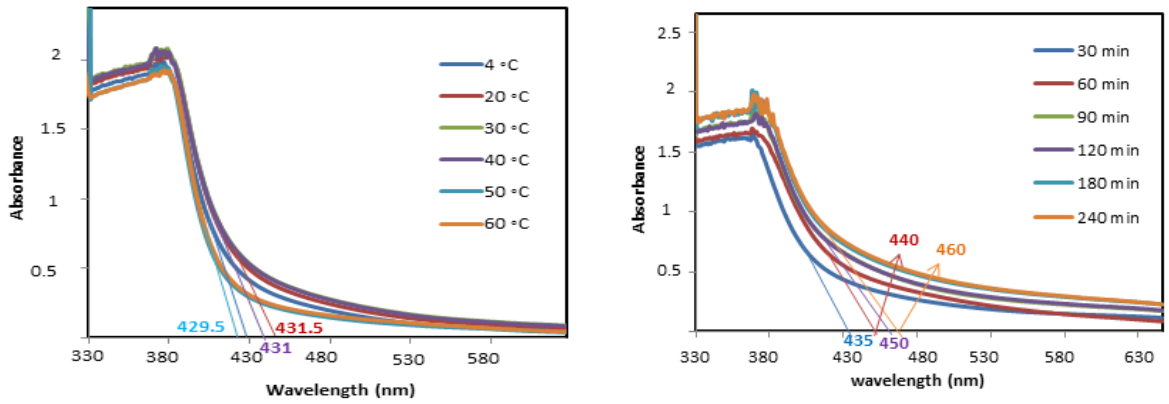

Figure 13. Estimation of the absorption edge wavelengths

The value of bandgap ZnO changes with the type of synthesis, preparation conditions, and particle dimensions. The results of the optical bandgap calculations are presented in Table 1. In this table, the results of the optical band gap are given only for different temperatures and times. Optimal conditions of synthesis have been considered, as well.

Table 1. The bandgap value estimated for different temperatures and times

Time (min)	E_g (eV)	Temperature (◦C)	E_g (eV)
30	2.727	4	2.886
60	2.613	20	2.876
90	2.298	30	2.876
120	2.298	40	2.879
180	2.177	50	2.889
240	2.177	60	2.889

According to the results of Table 1, the values of E_g are a function of the reaction time rather than the reaction temperature. The range of bandgap at different temperatures is almost constant, while it varies at different times. All of these values are different from the direct bandgap of ZnO. According to Figure 7, the main absorption peak has shifted to a higher wavelength. This redshift may be attributed to the presence of foreign materials in the lattice that affect the bandgap [64]. As can be seen from Table 1, when reaction time increases, the bandgap decreases accordingly. Also, the decrease in bandgap may be due to the presence of crystal defect and the quantum confinement effects. In this work, the presence of the plant as a reducing agent may have led to the redshift. Several researchers reported that the size of nanoparticles also attributes to bandgap [62, 63] and reaction time [61].

Evaluation of antibacterial properties

Several studies have shown the antibacterial activity of metal oxides. This activity is attributed to their stability at high temperatures and pressures [67]. In this regard, ZnO nanoparticles were known as strong antibacterial agents [68–72]. Also, several studies have reported antibacterial properties of the genus of Tragopogon [15, 19, 25]. In this research, based on previous studies, synthesized nanoparticles with Tragopogon graminifolius DC extract were expected to have antibacterial properties. Also, we investigated the antibacterial potential of the nanoparticles and extract against Gram-positive bacteria Staphylococcus aureus (S. aureus) and Gram-negative bacteria Escherichia coli (E. coli). The results showed the good antibacterial properties of the samples against these two bacteria. When the concentration of samples increases, the bactericidal property also increases against the bacteria strain (Figure 14). Time-kill assay [71] was performed using bacterial suspensions by adding different concentrations of plant extract and biosynthesized ZnO nanoparticles (0.01, 0.1, 0.5, 1, and 1.5%). Figure 13 shows that most of S. aureus bacteria were killed in the presence of plant extract after 24 h. In this experiment, the plant extract performance seems slightly better than that of the biosynthesized ZnO nanoparticles. In most studies reported, the bactericidal ability of extracts was attributed to aromatic and saturated molecules such as phenolic compounds, flavonoids, terpènes, and some other materials [68, 73]. In the present work, the mentioned compounds were reported based on the results of the FT-IR spectrum in the plant extract. These compounds are assumed to have the ability to inhibit bacterial growth and destroy their cell membranes by forming complexes with proteins [68]. Certainly, biosynthesized ZnO nanoparticles have also significant bactericidal ability. High surface area and small particle size of nanoparticles are two factors that inhibit bacterial growth [69, 74]. According to optical density (OD) analysis, the maximum amount of the bactericidal property was evaluated at a 1.5% concentration of biosynthesized ZnO nanoparticle and plant extract so that about 97.8% of the bacteria were destroyed. Tables 2 and 4 and Figure 15 illustrate the changes in the optical density of biosynthesized ZnO nanoparticles and plant extract. Based on Tables 3 and 5, it can be stated that the antibacterial ability of plant extract is slightly higher than the antibacterial ability of biosynthesized ZnO nanoparticles. Also, biosynthesized ZnO nanoparticles and plant extract had a greater effect on Gram-positive bacteria S. aureus. These results are consistent with the research of Ahmar Rauf and colleagues [75].

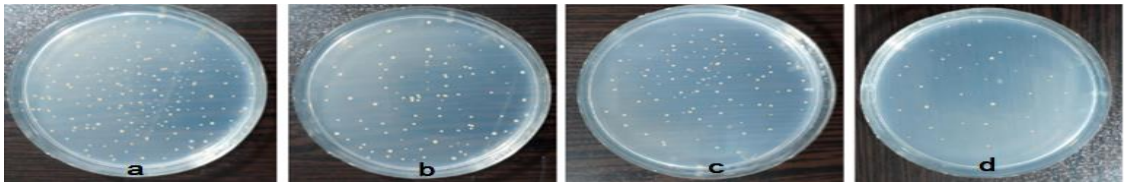

Figure 14. S. aureus bacteria in contact with biosynthesized ZnO nanoparticles and plant extract: a) Control group for ZnO nanoparticles, b) in the presence of biosynthesized ZnO nanoparticles, c) Control group for extract, and d) In the presence of plant extract

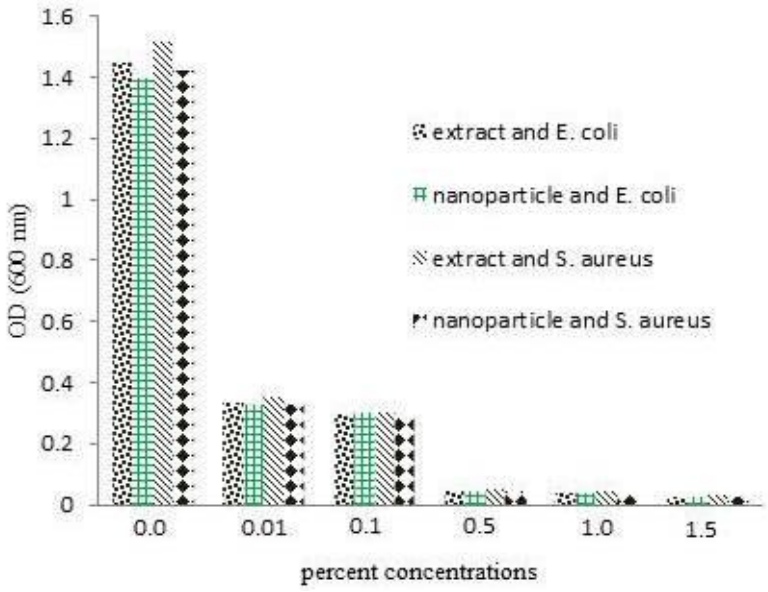

Figure 15. The effect of different concentrations of ZnO nanoparticles and plant extract on S. aureus and E. coli bacteria

Table 2. The changes in the optical density of the examined bacteria at different concentrations of biosynthesized ZnO nanoparticles

Bacteria	Control	0.01%	0.1%	0.5%	1%	1.5%
S. aureus	1.421	0.331	0.291	0.0485	0.0394	0.0305
E. coli	1.401	0.331	0.3025	0.048	0.0405	0.0305

Table 3. The changes in the optical density of the examined bacteria at different concentrations of Tragopogon graminifolius DC extract

Bacteria	Control	0.01%	0.1%	0.5%	1%	1.5%
S. aureus	1.521	0.356	0.305	0.051	0.046	0.0321
E. coli	1.452	0.3356	0.296	0.049	0.0425	0.0315

Table 4. The lethality of biosynthesized ZnO nanoparticles compared to the control group

Bacteria	0.01%	0.1%	0.5%	1%	1.5%
S. aureus	74.95	79.52	96.58	97.73	97.85
E. coli	76.37	78.41	96.57	97.11	97.82

Table 5. The lethality of Tragopogon graminifolius DC extract compared to the control group

Bacteria	0.01%	0.1%	0.5%	1%	1.5%
S. aureus	76.59	79.95	96.64	96.97	97.89
E. coli	76.89	79.61	96.62	97.07	97.83

Conclusions

In recent years, the synthesis of green nanoparticles has emerged as an eco-friendly nanotechnological method. Plants can act as reducers and stabilizers in the process of green synthesis because of their special compounds. In this research, a simple method is proposed to biosynthesize ZnO nanoparticles by Tragopogon graminifolius DC extract, which is an effective antioxidant. The pH, the concentration of zinc acetate dihydrate solution, the volume of plant extract, temperature, and contact time of zinc acetate dihydrate solution with plant extract were demonstrated as factors controlling the biosynthesis of ZnO nanoparticles. The synthesized nanoparticles were characterized by UV-Vis, XRD, FT-IR, and SEM techniques. Optical analysis of the ZnO nanoparticles spectrum demonstrates their optical properties and thus the necessity of investigating their photocatalytic properties. ZnO nanoparticles and plant extract have potential bactericidal activity against S. aureus and E. coli. The antibacterial activity can be due to interaction nanoparticles or plant extract with the cell membrane of bacteria. Finally, it can be said that Tragopogon graminifolius DC extract is an effective agent for the synthesis of ZnO nanoparticles that can also be used for the preparation of other metallic nanoparticles. Overall, it is hoped that the use of green nanoparticles can prevent the spread of some bacteria.

Acknowledgments

This work was supported by Islamic Azad University, Korramabad Branch.

Disclosure Statement

No potential conflict of interest was reported by the authors.

Orcid

Ghazaleh Kouchakzadeh 0000-0002-5358-8704

References

[1]. Nithya K., Kalyanasundharam S. *OpenNano*, 2019, **4**:100024
[2]. Noorjahan C.M. *Asian Journal of Pharmaceutcal and Clinical Research*, 2019, **12**:106
[3]. Saptarshi S.R., Duschl A., Lopata A.L. *Journal of nanobiotechnology*, 2013, **11**:1
[4]. Faddah L.M., Abdel Baky N.A., Al-Rasheed N.M., Al-Rasheed N.M., Fatani A.J., Atteya M. *BMC Complement Altern Med*., 2012, **12**:60
[5]. El Shemy M.A., Ibrahim Azab N., Fawzy Salim R. *Biophysics & Molecular Biology*., 2017, **2**:1
[6]. Sperling R.A., Zhang F., Zanella M., Parak W.J. *Chemical Society Reviews*., 2008, **37**:1896
[7]. Shobha N., Nanda N., Giresha A.S., Manjappa P., Dharmappa K.K., Nagabhushana B.M. *Materials Science and Engineering: C*., 2019, **97**:842
[8]. Shankar S.S., Rai A., Ahmad A., Sastry M. *Journal of Colloid and Interface Science*., 2004, **275**:469
[9]. Gour A., Kumar Jain N. *Nanomedicine, and Biotechnology*, 2019, **47**:844
[10]. Mali V.C., Ranger K., Lavate R.A., Kumbhar D.A., Sathe S.S., Kokare B.N. *Proceeding of Internatinal Conference on Advances in Materials Science*, 2016, **24**:648
[11]. Sumner L.W., Lei Z., Nilolau B.J., Saito K. *Natural Product Reports*., 2015, **32**:212
[12]. Agarwal H., Venkat Kumar S., Rajeshkumar S. *Resource- Efficient Technologies*, 2017, **3**:406

[13]. Santhoshkumar J., Venkat Kumar S., Rajesshkumar S. *Resource-Efficient Technologies*, 2017, **3**:459
[14]. Ezzatzadeh E., Hossaini Z., Varasteh Moradi A., Salimifard M., Afshari-Sharif Abad S. *Canadian Journal of Chemistry*, 2019, **97**:1
[15]. Heidari M., Bahramsoltani R., Abdolghaffari A.H., Rahimi R., Esfandyari M., Baeeri M., Hassanzadeh G., Abdollahi M., Farzaei M.H. *Journal of Traditional and Complementary Medicine*, 2019, **9**:54
[16]. Formisano C., Rigano D., Senatore F., Bruno M., Rosselli S. *Natural Product Research*, 2010, **24**:663
[17]. Sareedenchai V., Ganzera M., Ellmerer E.P., Lohwasser U., Zidorn C. *Biochemical Systematics and Ecology*, 2009, **37**:234
[18]. Farzaei M.H., Khazaei M., Abbasabadi Z., Feyzmahdavi M., Mohseni G.R. *Iranian Red Crescent Medical Journal*, 2013, **15**:813
[19]. Goorani S., Morovvati H., Seydi N., Zangeneh A., Zangeneh M.M. *Comparative Clinical Pathology*, 2019, **28**:435
[20]. Feyzmahdavi M., Khazaei M., Gholamin B., Abbasabadi Z. *Journal of Reports in Pharmaceutical Sciences*, 2017, **6**:161
[21]. Sadeghi A., Bahramsoltani R., Rahimi R., Farzaei M.H., Farzaei F., Minoosh Z., Haghghi S., Abdollahi M. *Journal of Dietary Supplements*, 2018, **15**:197
[22]. Farzaei M.H., Ghasemi-Niri S.F., Abdolghafari A.H., Baeeri M., Khanavi M., Navaei-Nigjeh M., Abdollahi M., Rahimi R. *Pharmaceutical Biology*, 2015, **53**:429
[23]. Zangeneh M.M., Salmani S., Zangeneh A., Khedri R., Zarei M.S. *Comparative Clinical Pathology*, 2019, **28**:1197
[24]. Al-Rimawi F., Rishmawi S., Ariqat Sh.H., Khalid M.F., Warad E., Salah Z. *Complementary and Alternative Medicine*, 2016, **2**:1
[25]. Seifpour R., Nozari M., Pishkar L. *Journal of Inorganic and Organometallic Polymers and Materials*, 2020, **30**:2926
[26]. Kroschewsky J.R., Mabry T.J., Markham K.R., Alston R.E. *Phytochemistry*, 1969, **8**:1495
[27]. Kucekova Z., MLcek J., Humpolicek P., Rop O., Valasek P., Saha P. *Molecules*, 2011, **16**:9207
[28]. Farzaei M.H., Rahimi R., Attar F., Siavoshi F., Saniee P., Hajimahmoodi M., Mirnezami T., Khanavi M. *Natural Product Communication*, 2014, **9**:121
[29]. Britton H.T.S., Robinson R.A. *Journal of the Chemical Society (Resumed)*, 1931, **0**:1456
[30]. Brand-Williams W., Cuvelier M.E., Berset C. LWT- *Food Science and Technology*, 1995, **28**:25
[31]. Katalinik V., Milos M., Kulisic T., Jukic M. *Food Chemistry*, 2006, **94**:550
[32]. Choi C.W., Kim S.C., Hwang S.S., Choi B.K., Ahn H.J., Lee M.Y., Park S.H., Kim S.K. *Plant Science*, 2002, **163**:1161
[33]. Behravan M., Hossein Panah A., Naghizadeh A., Ziaee M,. Mahdavi R., Mirzapour A. *International Journal of Biological Macromolecules*, 2019, **124**:148
[34]. Seifi Mansour S., Ezzatzadeh E., Safarkar R. *Asian Journal of Green Chemistry*, 2019, **3**:353
[35]. Villanueva M.E., Cuestas M.L., Pérez C.J, Dall´ Orto V.C., Copello G.J. *Journal of Colloid and Interface Science*, 2019, **536**:372
[36]. Baek S., Hee Joo S., Toborek M. *Journal of Hazardous Materials*, 2019, **373**:122
[37]. Iravani S., *Green Chemistry*., 2011, **13**:2638
[38]. Jamzad M., Karami Bidkorpeh M. *Journal of Nanostructure in Chemistry*, 2020, **10**:193
[39]. Hosseini Koupaei M., Shareghi B., Saboury A. A., Davat F., Semnani A., Evini M. *Royal Society of Chemistry Advances*, 2016, **6**:42313
[40]. Marja P., Hopia A.I., Vuorela H.J., Rauha J., Pihlaja K., Kujala T.S., Heinonen M. *Journal of Agriculture Food Chemistry*, 1999, **47**:3954
[41]. Blainski A., Lopes G.C., Palazzo de Mello J. C. *Molecules*, 2013, **18**:6852
[42]. Li X., Wu X., Huang L. *Molecules*, 2009, **14**:5349
[43]. Chandra Shekhar T., Anju G. *American Journal of Ethnomedicine*, 2014, **1**:244

[44]. Huong D.Q., Duong T., Cam Nam P. *Vietnam Journal Chemistry*, 2019, **57**:469
[45]. Ansari M.A., Murali M., Prasad D., Alzohairy M.A., Almatroudi A., Alomary M.N., Udayashankar A.C., Singh S.B., Asiri S.M., Ashwini B.S., Gowtham H.G., Kalegowda N., Amruthesh K.N., Lakshmeesha T.R., Niranjana S.R. *Biomolecules*, 2020, **10**:336
[46]. Ambrožič G., Crnjak Oral Z., Žigon M., *Materials and technology*, 2011, **43**:173
[47]. Ezealisiji K.M., Siwe-Noundou X., Maduelosi B., Nwachukwu N., Maçedo Krause R. W. *International Nano Letters*, 2019, **9**:99
[48]. Basnet P., Inakhunbi Chanu T., Samanta D., Chatterjee S. *Journal of Photochemistry and Photobiology*, 2018, **183**:201
[49]. Malek Mohammadi F., Ghasemi N. *Journal of Nanostructure in Chemistry*, 2018, **8**:93
[50]. Jain P.K., Huang X., El-Sayed I.H., El-Sayed M. A. *Plasmonics*, 2007, **2**:107
[51]. Khalil M.M.H., Ismail E.H., El-Baghdady K.Z., Mohamed D. *Arabian Journal of Chemistry*, 2014, **7**:1131
[52]. Buazar F., Bavi M., Kroushawi F., Halvani M., Khaledi-Nasab A., Hossieni S.A. *Journal of Experimental Nanoscience*, 2016, **11**:175
[53]. Rafaie H., Samat N., Nor R.M. *Materials Letters*, 2014, **137**:297
[54]. Moezzi A., Cortie M., Mc Donagh A. *Royal Society of Chemistry*, 2011, **40**:4871
[55]. Rodríguez-Paéz J.E., Caballero A.C., Villegas M., Moure C., Durán P., Fernández J.F. *Journal of the European Ceramic Society*, 2001, **21**:925
[56]. Nithya K., Kalyanasundharam S. *Open Nano*, 2019, **4**:100024
[57]. Dinesh V.P., BiJi P., Ashok A., Dhara S.K., Kamaruddin M., Tyagi A.K., Raj B. *Electronic Supplementary Material (ESl) for RSC Advances*, 2014, **4**:58930
[58]. Bouzourâa M., En Naciri A., Moadhen A., Rinnert H., Guendouz M., Battie Y., Chaillou A., Zaïbi M.A. *Materials Chemistry and Physics*, 2016, **175**:233
[59]. Nagarajan S., Kuppusamy K.A. *Journal of Nanobiotechnology*, 2013, **11**:39
[60]. Gnanasangeetha D., Thambavani D.S. *Journal of Chemical, Biological and Physical Sciences*, 2014, **4**:238
[61]. Wasly H.S., El-Sadek M.S.A., Henini M. *Applied Physics A: Materials Science & Processing*, 2018, **124**:76
[62]. Wang Z.L. *ACS Nano*, 2008, **2**:1987
[63]. Debanath M.K., Karmakar S. *Materials Letters*, 2013, **111**:116
[64]. Pudukudy M., Yaakob Z. *Journal Cluster Science*, 2014, **26**:1187
[65]. Charles K. *Introduction to Solid States Physics*. Eighth Edition, New York: Wiley, 2005
[66]. Singh J., Kaur S., Kaur G., Basu S., Rawat M. *Green Process Synthesis*, 2019, **8**:272
[67]. Bouazza A., Bassaid S., Daho B., Messori M., Dehbi A. *Polymers and Polymer Composites*, 2021, **29**:417
[68]. Thi T.U.D., Nguyen T.T., Thi Y.D., Thi K.H.T., Phan B.T., Pham K.N. *Royal Society of Chemistry Advances*, 2020, **10**:23899
[69]. Awwad A.M., Amer M.W., Salem N.M., Abdeen A.O. *Chemistry International*, 2020, **6**:151
[70]. Pillai A.M., Sivasankarapillai V.S., Rahdar A., Joseph J., Sadeghfar F., Anuf A.R., Rajesh K., Kyzas G. *Journal of Molecular Structure*, 2020, **1211**:128107
[71]. Fahimmunisha B.A., Ishwarya R., AlSalhi M.S., Devanesan S., Govindarajan M., Vassehran B. *Journal of Drug Delivery Science and Technology*, 2020, **55**:101465
[72]. Yusof H.M., Mohamah R., Zaidan U.H., Abdul Rahman N.A. *Journal of Animal Science and Biotechnology*, 2019, **10**:57
[73]. Zhang L., Jiang Y., Ding Y., Daskalakis N.N., Jeuken L.J.C., Povey M.J., O' Neill A.J., York D.Y. *Journal of Nanoparticle Research*, 2010, **12**:1625
[74]. Vijayakumar S., Arulmozhi P., Kumar N., Sakthivel B., Prathip Kumar S., Praseetha P.K. *Materials Today: Proceedings*, 2019, **23**:73

[75]. Ahmar Rauf M., Owais M., Rajpoot R., Ahmad F., Khan N., Zubair S. *Royal Society of chemistry Advsnced*, 2017, **7**:36361

How to cite this manuscript: Marzieh Naderi, Ghazaleh Kouchakzadeh*. The ability of Tragopogon graminivorous DC *edible* medicinal plant for optimum synthesis of zinc oxide green nanoparticles and evaluation of antibacterial properties of its extract and nanoparticles. *Asian Journal of Nanosciences and Materials*, 4(4) 2021, 290-308.
DOI:10.26655/AJNANOMAT.2021.4.5